Biogeosciences Discuss., doi:10.5194/bg-2017-148, 2017
Manuscript under review for journal Biogeosciences
Discussion started: 21 April 2017


Biogeosciences Discussions Open Access EGU

# Low $pCO_2$ under sea-ice melt in the Canada Basin of the western Arctic Ocean

Naohiro Kosugi[1], Daisuke Sasano[2], Masao Ishii[1], Shigeto Nishino[3], Hiroshi Uchida[3], Hisayuki Yoshikawa-Inoue[4]

[1]Meteorological Research Institute, Tsukuba, 305-0052, Japan
[2]Japan Meteorological Agency, Tokyo, 100-8122, Japan
[3]Japan Agency for Marine-Earth Science and Technology, Yokosuka, 237-0061, Japan
[4]Hokkaido University, Sapporo, 060-0810, Japan

*Correspondence to*: Naohiro Kosugi (nkosugi@mri-jma.go.jp)

**Abstract.** In September 2013, we observed an expanse of surface water with low $CO_2$ partial pressure ($pCO_2^{sea}$) (< 200 μatm) in the Chukchi Sea of the western Arctic Ocean. The large undersaturation of $CO_2$ in this region was the result of massive primary production after the sea-ice retreat in June and July. In the surface of the Canada Basin, salinity was low (< 27) and $pCO_2^{sea}$ was closer to the air–sea $CO_2$ equilibrium (~360 μatm). From the relationships between salinity and total alkalinity, we confirmed that the low salinity in the Canada Basin was due to the larger fraction of meltwater input (~0.16) rather than the riverine discharge (~0.1). We attribute the relatively high $pCO_2^{sea}$ in the Canada Basin to the shallow mixed layer and limited net primary production. Such an increase in $pCO_2^{sea}$ was not so clear in the coastal region near Point Barrow, where the fraction of riverine discharge was larger than that of sea ice melt. We also identified low $pCO_2^{sea}$ (< 250 μatm) under the halocline of the Canada Basin. Oxygen supersaturation in this subsurface layer corroborates that the decrease in $pCO_2^{sea}$ was due to net primary production. If these low $pCO_2^{sea}$ layers surface by wind mixing, they will act as additional $CO_2$ sinks; however, this is unlikely because intensification of stratification by sea-ice melt inhibits mixing across the halocline.

## 1 Introduction

The extent of sea ice and its thickness in the Arctic Ocean have been declining in recent decades (e.g., Comiso, 2012; Stroeve et al., 2012a, 2012b); these declines are widely considered a consequence of climate change resulting from the emissions of anthropogenic greenhouse gases. The average monthly extent of sea ice in September in the Arctic Ocean decreased by about 12.4% per decade from 1979 to 2010 (Stroeve et al., 2012b). In September 2012, the area of sea ice in the Arctic Ocean was less than $4 \times 10^6$ km$^2$, about 50% of the average in the 1980s (Parkinson and Comiso, 2013). Because of this decline in the extent of sea ice, the air–sea $CO_2$ flux in the Arctic Ocean is also thought to be dramatically changing. Currently, the Arctic $CO_2$ sink has been estimated as 66–199 Tg C yr$^{-1}$, with a large uncertainty (Bates and Mathis, 2009). This value is equivalent to 3–8% of the net $CO_2$ sink of the global ocean (2.6 ± 0.5 Pg C yr$^{-1}$ in the period 2006–2015; Le

Biogeosciences Discuss., doi:10.5194/bg-2017-148, 2017
Manuscript under review for journal Biogeosciences
Discussion started: 21 April 2017


Quéré et al., 2016). A recent modeling study suggests that the $CO_2$ sink in the Arctic Ocean is increasing (Manizza et al., 2013).

The reasons for an increasing $CO_2$ sink in the Arctic Ocean include the increase in the area and duration of ice-free conditions and the enhanced net primary production they induce. However, the effect of increasing meltwater input that accompanies the sea ice decline should also be taken into consideration (e.g., Yamamoto-Kawai et al., 2009; Rabe et al., 2014). The large input of ice melt enhances stratification in the upper layer and forms a thin surface mixed layer with a distinct halocline below. Although dilution of the surface water with meltwater lowers the partial pressure of $CO_2$ ($pCO_2^{sea}$), shoaling of the surface mixed layer would accelerate equilibration of the surface water with the overlying air. The input of meltwater is also likely to influence carbonate chemistry by altering the ratio of dissolved inorganic carbon (DIC) to total alkalinity (TA), although it is still unclear whether the addition of meltwater increases or decreases the DIC/TA ratio (Rysgaard et al., 2007; Bates et al., 2014). Cai et al. (2010) reported unprecedented high $pCO_2^{sea}$ (~370 µatm) in the Canada Basin in summer. They ascribed this high $pCO_2^{sea}$ to low net primary production and rapid equilibration with atmospheric $CO_2$ in the shallow mixed layer derived from meltwater input. The low nutrient content in meltwater reduces the biological drawdown of $pCO_2^{sea}$. Else et al. (2013) found that surface warming also contributed significantly to $pCO_2^{sea}$ increase in a shallow mixed layer in the Canada Basin. Both studies concluded that an increase in meltwater lowers $CO_2$ absorbing capacity in the Canada Basin.

A notable feature of the Canada Basin in summer is a complex water column structure. Because of the strong salinity gradient, there are several maxima and minima of temperature within 150 m of the surface. This water column structure does not always remain stable in the rapidly changing Arctic Ocean. Although Cai et al. (2010) and Else et al. (2013) reported relatively high surface $pCO_2^{sea}$ in the Canada Basin, they did not fully explain the $CO_2$ chemistry below the surface mixed layer there. We studied the water column $CO_2$ variation in the western Arctic Ocean and the processes that cause it.

In late summer 2013, we made shipboard observations in the Chukchi Sea and in the Canada Basin of the western Arctic Ocean. While underway or at hydrographic stations, or both, we measured temperature, salinity, dissolved oxygen, and the carbonate system variables $pCO_2^{sea}$, DIC, and TA. From the salinity–TA relationship, we also mapped the mixing ratio of sea-ice meltwater, riverine outflow, and a water of Pacific origin that entered into the western Arctic Ocean through the Bering Strait. The results demonstrate the importance of large net primary production in reducing the $pCO_2^{sea}$ and increasing air-to-sea $CO_2$ flux in the Chukchi Sea. Although this low $pCO_2^{sea}$ water is advected into the Canada Basin, air-to-sea $CO_2$ flux there is blocked by a stratified shallow surface layer that is formed by a large ice-melt input.

## 2. Data and Methods

Oceanographic measurements in the Chukchi Sea and the Canada Basin were made during cruise MR13-06 of the R/V *Mirai* conducted by the Japan Agency for Marine-Earth Science and Technology from 28 August to 6 October 2013

Biogeosciences Discuss., doi:10.5194/bg-2017-148, 2017
Manuscript under review for journal Biogeosciences
Discussion started: 21 April 2017


(Nishino et al., 2015). The data used in this paper are available from the JAMSTEC Data Site for Research Cruises (http://www.godac.jamstec.go.jp/darwin/cruise/mirai/mr13-06_leg1/e).

We made underway measurements of $pCO_2^{sea}$ and DIC together with temperature ($T$) and salinity ($S$) in seawater pumped continuously from an intake located 4.5 m below surface. For the measurement of $pCO_2^{sea}$, the pumped water was continuously introduced into a shower-type equilibrator with 1.4 $dm^3$ headspace at a rate of 4 $dm^3$ $min^{-1}$. A wavelength-scanned cavity ring-down spectrometer (Picarro G2301, Picarro Inc., USA) was used to measure the concentrations of $CO_2$ in the headspace of the equilibrator and in the atmosphere (sampled from the foremast). The instrument was calibrated once a day against a set of three working standard gases of $CO_2$ in air (Japan Fine Products, 206 to 489 ppmv) that had been standardized on the WMO scale. Surface $pCO_2^{sea}$ was calculated from the mole fraction of $CO_2$ in the air by taking the water vapor pressure and atmospheric pressure into account. The temperature and salinity of the pumped water at the intake were continuously measured with sensors SBE 38 and SBE 45, respectively (Sea-Bird Electronics, USA). PT100 thermometer was equipped with the equilibrator. An increase in temperature between in situ seawater ($T_{in}$) and the equilibrator ($T_{eq}$) was typically about 0.2 °C. Equation (1) proposed by Takahashi et al. (2009) was applied to convert $pCO_2(T_{eq})$ to $pCO_2(T_{in})$,

$$pCO_{2(Tin)} = pCO_{2(Teq)} \times \exp\left[0.0433(T_{in} - T_{eq}) - 4.35 \times 10^{-5}\left\{(T_{in})^2 - (T_{eq})^2\right\}\right] \quad (1)$$

Uncertainty in the value of $pCO_2^{sea}$ measured using the same type of equilibrator has been estimated to be ±3 µatm (Midorikawa et al., 2006).

Air–sea $CO_2$ flux ($F_{CO2}$) was calculated using the following equation:

$$\Delta pCO_2 = pCO_2^{sea} - pCO_2^{air} \quad (2)$$

$$F_{CO2} = k\alpha\Delta pCO_2 \quad (3)$$

where α denotes the solubility of $CO_2$ in seawater (Weiss 1974). We used a gas-transfer piston velocity $k$ given by Wanninkhof (1992):

$$k = \{2.5(0.5246 + 1.6256 \times 10^{-2}t + 4.9946 \times 10^{-4}t^2) + 0.3 \times U_{10}^2\} \times (Sc/660)^{-0.5} \quad (4)$$

$t$, $U_{10}$, and $Sc$ denote temperature of seawater (in degrees Celsius), wind speed at 10 m above sea level, and the Schmidt number, respectively. An anemometer was located on the foremast at 24 m above sea level. $U_{10}$ was determined by multiplying the wind speed measured by the anemometer by $(10/24)^{0.11}$ (Hsu et al., 1994).

For the underway measurement of DIC, a portion of pumped water was taken and filled automatically into glass bottles (SCHOTT DURAN®; 300 $cm^3$) every 15 minutes. DIC was measured after the temperature of the sample seawater was adjusted to 20.0 °C in a thermostated water bath for 1 hour, using a $CO_2$ extraction/coulometric titration system (Nippon ANS, Japan). The system was standardized with Certified Reference Material (CRM; Batch #113) supplied by A. G. Dickson (Scripps Institution of Oceanography); underway measurement of DIC was interrupted for several hours once a day for calibration. The precision of measurement determined by repeatability of CRMs was ±2.2 µmol $kg^{-1}$. The values of TA in the surface were calculated from $pCO_2^{sea}$, DIC, temperature and salinity using dissociation constants of carbonic acid given by Lueker et al. (2000). Uncertainty in surface TA was estimated as ±3 µmol $kg^{-1}$ by taking the uncertainties of DIC and $pCO_2^{sea}$ into account.

Biogeosciences Discuss., doi:10.5194/bg-2017-148, 2017
Manuscript under review for journal Biogeosciences
Discussion started: 21 April 2017




At hydrographic stations, seawater column profiles of temperature, salinity, and dissolved oxygen were obtained with a CTD (SBE 9 plus, Sea-Bird Scientific, USA) rosette sampler equipped with sensors for dissolved oxygen (SBE 43, Sea-Bird Scientific, USA) and Niskin bottles (12 $dm^3$). In addition to the CTD casts, some expendable CTDs (XCTD) were used to obtain column profiles of temperature and salinity. Discrete water samples were taken into Niskin bottles at depths along with CTD measurements. Measurements of dissolved oxygen were made by the Winkler titration method following Dickson (1994) and used to correct for the bias of the data from the oxygen sensor SBE 43. Apparent oxygen utilization (AOU), *i.e.*, the difference between the measured concentration of dissolved oxygen and its saturation concentration under the same physical conditions, was calculated using the oxygen solubility constant given by Garcia and Gordon (1992). Water samples for chlorophyll a were vacuum-filtered (< 0.02 MPa) through a 25-mm-diameter Whatman grade GF/F filter, and fluorescence was measured for each sample with a fluorometer (10-AU-005, Turner Designs, USA).

Subsamples for DIC and TA measurements in the discrete water samples were drawn into borosilicate glass bottles (300 $cm^3$ for DIC and 125 $cm^3$ for TA) using the protocol of Dickson et al. (2007). Measurements of DIC at depths were also made with the extraction/coulometric system (Nippon Ans., Japan). Saturated solution of $HgCl_2$ (0.1 $cm^3$) was added to each of the samples to inhibit any biological activity. Measurements of TA were made with a spectrophotometric system (Nippon Ans., Japan) based on a single-point pH determination using bromocresol green as an indicator dye (Yao and Byrne, 1998). Replicate measurements yielded an average and standard deviation of differences of 1.0 ± 1.1 μmol $kg^{-1}$ for DIC and 0.9 ± 0.8 μmol $kg^{-1}$ for TA. Values of $pCO_2^{sea}$ in discrete water samples were calculated from DIC, TA, temperature, and salinity using dissociation constants of carbonic acid given by Lueker et al. (2000).

## 3. Results and Discussion

### 3.1. Mixing ratio of Pacific-origin, ice-melt, and riverine waters

In the western Arctic Ocean, the water at the temperature minimum layer (~150 dbar) is known to originate in the North Pacific and be advected into the Arctic through the Bering Strait (POW: Pacific Origin Water, Shimada et al., 2005), and the water in the layer above the temperature minimum is thought to be a mixture of this POW with sea-ice melt and riverine outflow. To determine the fractions ($f$) of the three different source waters — POW, sea-ice melt (SIM), and riverine outflow (RRO) — in the upper-layer waters of the Chukchi Sea and the Canada Basin, we used the relationship between salinity and TA and the following mass balance equations.

$$TA = f_{POW} \cdot TA_{POW} + f_{SIM} \cdot TA_{SIM} + f_{RRO} \cdot TA_{RRO} \quad (5)$$

$$S = f_{POW} \cdot S_{POW} + f_{SIM} \cdot S_{SIM} + f_{RRO} \cdot S_{RRO} \quad (6)$$

$$1 = f_{POW} + f_{SIM} + f_{RRO} \quad (7)$$

We chose the data of TA and $S$ from 38 sampling layers/locations in the temperature minimum layer where $T$ < -1.5 °C in the Chukchi Sea and the Canada Basin during the cruise, and defined their means (2264.2 ± 12.6 μmol $kg^{-1}$ and 32.89 ± 0.22) as the values of $TA_{POW}$ and $S_{POW}$, respectively (Fig. 1).

Biogeosciences Discuss., doi:10.5194/bg-2017-148, 2017
Manuscript under review for journal Biogeosciences
Discussion started: 21 April 2017




There are several studies of TA of riverine outflow in the Arctic. Cooper et al. (2008) directly measured TA in six major rivers in the Arctic: they concluded that flow-weighted average of TA of these six rivers was 1048 μmol $kg^{-1}$. Yamamoto-Kawai et al. (2009) made linear regression analysis of salinity and TA, and reported that the intercept ($S$ = 0) was 793 μmol $kg^{-1}$ for the whole Canada Basin. Data of TA and salinity taken during our cruise indicate that the upper limit of distribution in salinity-TA plots (Fig. 2) is consistent with the line extended to this intercept deduced by Yamamoto-Kawai et al. (2009); consequently, we regarded this value as $TA_{RRO}$. In consideration of the spatial and temporal fluctuation of riverine TA, we assumed that the uncertainty of TARRO is ±100 μmol $kg^{-1}$ (Yamamoto-Kawai et al., 2005). Accordingly, the estimated errors of $f_{SIM}$ and $f_{RRO}$ are as large as ±0.02.

Conversely, values of $S_{SIM}$ and $TA_{SIM}$ so far reported fall within a relatively narrow range. We applied $S_{SIM}$ = 5 and $TA_{SIM}$ = 349 μmol $kg^{-1}$ following Fransson et al. (2009). Differences in $f_{SIM}$ and $f_{RRO}$ are not larger than ±0.008 when applying other values suggested by Anderson et al. (2004) ($S_{SIM}$ = 4, $TA_{SIM}$ = 263 μmol $kg^{-1}$). Cumulative error in $f_{SIM}$ and $f_{RRO}$ associated with the selection of the end-member salinity and TA are within ±0.03. As shown in Fig. 2, $S$–TA plots for the Chukchi Sea and Canada Basin fall among the three $S$–TA end-members of POW, SIM, and RRO. Surface water in the Chukchi Sea and Canada Basin consists mainly of POW, but includes sizable $f_{SIM}$ up to 0.16 and $f_{RRO}$ up to 0.18.

### 3.2. Variations in Temperature and Salinity in the Surface Layer

In the period from 4 to 11 September 2013, temperature (SST), salinity (SSS), $pCO_2^{sea}$, and DIC in surface water were highly variable in the western Arctic Ocean (Fig. 3), particularly around the continental slope (200 m isodepth in Fig. 3) of the Chukchi Sea. Average $pCO_2^{air}$ measured onboard was 385.0 μatm, which is consistent with the value observed at Point Barrow, Alaska (http://ds.data.jma.go.jp/gmd/wdcgg/). Average $U_{10}$ in the region north of 70°N was 7.2 m $s^{-1}$ during the cruise.

Variation in SST and SSS on the cruise track was abrupt rather than gradual (Fig. 3a and 3b). Therefore, we defined three subregions depending on SST and SSS as follows. (1) Barrow Coastal Water (BCW) was relatively warm and fresh (SST > 2 °C, SSS < 30.5). (2) Canada Basin Water (CBW) was cold and fresh (SST < 2 °C, SSS < 28). (3) Chukchi Sea Water (CSW) was saline (SSS > 28). The boundary between BCW and CBW was located at 72.5°N, 154.8°W. That between CBW and CSW was at 73.3°N, 168.3°W (Fig. 3c).

The fraction of freshwater had distinct spatial variations among the three subregions (Fig. 3d and 3e; summarized in Table 1). Low salinity in BCW was mainly due to riverine outflow: in this subregion, $f_{RRO}$ was as large as 0.18, presumably because the Alaskan coastal current which flows northward along the Alaskan coast toward Point Barrow contains a considerable fraction of Yukon River outflow (Steele et al., 2004). In contrast, the lower salinity in the CBW was primarily due to the input of meltwater from sea ice, although it also contained significant riverine outflow. In the northernmost region of the Canada Basin visited during the cruise (north of 74°N), $f_{SIM}$ was as large as 0.16, whereas $f_{RRO}$ was no more than 0.10 and was almost always lower than $f_{SIM}$. CSW was largely composed of Pacific water and rarely contained riverine outflow as it flowed directly from the Bering Strait.

Biogeosciences Discuss., doi:10.5194/bg-2017-148, 2017
Manuscript under review for journal Biogeosciences
Discussion started: 21 April 2017




### 3.3. Variations in carbonate chemistry in the Surface Layer

Remarkable differences in $pCO_2^{sea}$, DIC, and TA were observed among the three subregions (Table 1, Fig. 3f, g, and h). We attributed the low DIC/TA ratio and the resulting low $pCO_2^{sea}$ (< 200 µatm) in CSW to the massive biological activity there in early summer. In this region, net primary production decreases $pCO_2^{sea}$ to 200 µatm or less in early summer (Bates 2006). According to analyses of satellite imagery (Behrenfeld and Falkowski, 1997), net primary productivity (NPP) in July 2013 was as high as 1000 mgC $m^{-2}$ $day^{-1}$ in the majority of the Chukchi Sea. Even though NPP had decreased to ~500 mgC $m^{-2}$ $day^{-1}$ in September 2013 during our measurements, $pCO_2^{sea}$ had been notably lower than $pCO_2^{air}$ for months after the massive primary production in early summer, because of relatively slow gas exchange with the atmosphere: the half-life of $CO_2$ gas exchange, *i.e.*, the time required to reduce $\Delta pCO_2$ by half, was about 90 days under typical summer conditions ($T$ = 3 °C, $S$ = 32, TA = 2220 µmol $kg^{-1}$, mixed layer depth = 15 m, and $U_{10}$ = 7.2 m $s^{-1}$).

The DIC/TA ratio in CBW was higher than that in CSW (Table 1). The value of $pCO_2^{sea}$ in CBW ranged from 300 to 360 µatm (Fig. 3f). Although the level of $pCO_2^{sea}$ in CBW was still lower than the $pCO_2^{air}$ (385 µatm), it was much higher than that in CSW. The primary cause of the $pCO_2^{sea}$ being nearly as high as $pCO_2^{air}$ is that the addition of meltwater to the surface layer shoals the mixed layer (Cai et al., 2010; Else et al., 2013), thereby reducing the time for surface water to reach air–sea $CO_2$ equilibrium. An additional cause of higher $pCO_2^{sea}$ in the high $f_{SIM}$ region is probably low net primary production, because the concentrations of nutrients in meltwater are low; e.g., Lee et al. (2012) reported that the concentration of nitrate in a melt pond being formed on the top of sea ice in the Canada Basin was low (< 0.5 µM), and that the low nitrate concentration limited biological production in the pond. Our results corroborate previous reports by Cai et al. (2010) and Else et al. (2013) that the overspreading of the surface layer by sea-ice melt inhibits $CO_2$ uptake by the ocean. High $pCO_2^{sea}$ conditions after seasonal sea-ice retreat is likely to be common in the Canada Basin. The impact of sea-ice melt itself on $pCO_2^{sea}$ was difficult to resolve only from our observations. Bates et al. (2014) found both basic (i.e., DIC/TA < 1) and relatively acidic (i.e., DIC/TA > 1) melt ponds in the Canada Basin. To study the impact of meltwater on carbonate chemistry, direct sampling of sea ice into gastight bags (Fransson et al., 2013) will be required.

In BCW, $pCO_2$sea was about 270 µatm on average, between that in CSW and CBW (Fig. 3f). The fraction of freshwater indicates that surface freshening in BCW is mainly caused by riverine outflow ($f_{RRO}$ = 0.11) rather than sea-ice melt ($f_{SIM}$ = 0.08). Riverine outflow had a higher TA/$S$ ratio than sea-ice melt (Fig. 2). It also has larger content of DIC (Ulfsbo et al., 2014). In our measurements, surface chlorophyll *a* was higher in BCW (0.4 to 2.0 mg $dm^{-3}$) than in CBW (0.1 to 0.3 mg $dm^{-3}$), implying that biological drawdown of DIC was greater in BCW. Consequently, both DIC/TA and $pCO_2^{sea}$ in BCW were lower than those in CBW. Reduction in $CO_2$ absorption capacity by riverine discharge was not as large as that by sea-ice melt. This is an important finding, because river water inflow into the Arctic Ocean is considered highly likely to increase with climate change (McClelland et al., 2006; Déry et al., 2009).

Biogeosciences Discuss., doi:10.5194/bg-2017-148, 2017
Manuscript under review for journal Biogeosciences
Discussion started: 21 April 2017




### 3.4. Variations in the Water Column

Water properties among the three subregions differed not only in the surface but also in the water column. *T*-*S* diagrams obtained by CTD for each subregion are shown in Fig. 4. The surface around Point Barrow was fresh and warm; with depth, the water column gradually cooled to the coldest water around $S = 33$ (Fig. 4a). A similar decrease in temperature from near surface to bottom was observed in the Chukchi Sea (Fig. 4b). In contrast, the water column in the Canada Basin was more complex, with a number of temperature maxima and minima (Fig. 4c). Jackson et al. (2010) classified the water column in the Canada Basin from the top to bottom into a surface mixed layer, a near surface temperature maximum (NSTM), a remnant of the Winter Mixed Layer (rWML), Pacific Summer Water (PSW), and Pacific Winter Water (PWW). The surface mixed layer had the lowest salinity ($S < 27$) because almost all sea-ice melt is trapped in this layer during summer. The NSTM is separated from the surface mixed layer by stratification and warmed by the input of solar radiation. Below the NSTM, the rWML corresponded to the temperature minimum ($T = -1$ ℃, $S = 29.3$), which was formed in the Canada Basin during the previous winter. Another temperature maximum around S = 30.5 corresponded to PSW, which was advected and modified in the Chukchi Sea during summer. The lowest temperature observed was PWW near the freezing point and around $S = 33$.

Temperature and salinity were frequently observed along the cruise track by CTD and XCTD sensors. Column profiles included a distinct halocline from 10 to 20 dbar in BCW and CBW (Fig. 5a and 5b). In these two subregions, the salinity gradient from above the halocline to below it was up to 2. In CSW, the halocline, although not as clear as in the other two subregions, was at almost the same depth. Column variation of $f_{SIM}$ and $f_{RRO}$ indicate that both sea-ice meltwater and river outflow greatly affected the formation of the halocline (Fig. 5c and 5d). In the Canada Basin, $f_{SIM}$ was as high as 0.12 ± 0.01 (± standard deviation) in the top layer down to 10 dbar, but decreased abruptly with depth to practically zero (0.01 ± 0.01) in the 29–50 dbar layer. In contrast, $f_{RRO}$ was also quite high (0.09 ± 0.01) in the top layer down to 10 dbar and decreased gradually to 0.06 ± 0.02 in the 29–50 dbar layer. This vertical structure indicates that the input of sea-ice melt occurred shortly before the measurement (at least, in summer 2013) and contributed to the formation of a discrete layer in the surface over the main water mass in the Canada Basin, whereas river outflow had undergone vertical mixing in the course of advection before it reached the Canada Basin.

Among these three subregions, differences were also evident in column $pCO_2^{sea.}$ In the upper layer (above 10 dbar) of CSW and BCW, average $pCO_2^{sea}$ was 195 ± 11 µatm and 258 ± 14 µatm, respectively. As mentioned in section 3.2, these low $pCO_2^{sea}$ values were the result of net primary production. In these subregions, $pCO_2^{sea}$ increased with depth below the halocline. The column profile of AOU indicates that the increase in $pCO_2^{sea}$ was due to the input of $CO_2$ associated with the degradation of organic matter (Fig. 5e and 5f).

Unlike the column profiles of $pCO_2^{sea}$ and AOU in CSW and BCW, those in CBW were distinctive in that they had subsurface minima. In the top 10 dbar of CBW, $pCO_2^{sea}$ reached 322 ± 20 µatm, a value still lower than $pCO_2^{air}$ (~385 µatm) but the highest among the three subregions. However, $pCO_2^{sea}$ decreased with depth below the halocline and reached 271 ±

31 μatm in the range of 29.4 < *S* < 31.3 (30 to 50 dbar layer; Fig. 5e and 6a). Below the halocline in CBW, AOU was largely negative (~ –40 μmol $kg^{-1}$) like that in the CSW where net primary production was large (Fig. 5f and 6b).

Subsurface maxima of chlorophyll *a* and dissolved oxygen have also been found in the Canadian Archipelago (Martin et al., 2010). Here, our frequent observations facilitated classification of the water masses and their origins; this in turn explains the biological production in the subsurface layer of the Canada Basin. According to the salinity–AOU profile (Figure 6b) in the Canada Basin, AOU was negative (i.e., oxygen was saturated) in the range of 29.5 < *S* < 31.0 corresponding rWML and PSW. These water types were present in the 30–50 m depth layer (Fig. 5b). A column profile of photosynthetically active radiation in the Canada Basin shows that, although not strong, sunlight surely reaches the 50 m depth (Jackson et al., 2010); this sunlight fueled net primary production in the rWML with nutrients entrained during winter mixing. Oxygen supersaturation was greater in PSW than in rWML, even though PSW was deeper, probably because of massive primary production in the Chukchi Sea; the PSW there very likely subducted and advected into the Canada Basin before releasing all its excess oxygen to the atmosphere.

### 3.5. Future direction of hidden $CO_2$ sink in the Canada Basin

Predictions of the effects of a long-term retreat of sea ice on the air–sea $CO_2$ flux in the Arctic Ocean are contradictory. For example, Manizza et al. (2013) argued that increasing SST will enhance biological primary production and drawdown of $CO_2$. Laruelle et al. (2014) asserted that larger ice-free areas and longer ice-free periods will provide greater occasion for oceanic $CO_2$ uptake. In contrast, Cai et al. (2010) and Else et al. (2013) insisted that the increase in sea-ice melt results in the formation of thin surface mixed layers and limits further uptake of atmospheric $CO_2$ by this layer.

As a result of our observations that a subsurface minimum of $pCO_2^{sea}$ existed in the Canada Basin, it is necessary to study whether the surface mixed layer there will deepen under a warming climate. If the surface seawater is stirred by strong wind, the subsurface low $pCO_2^{sea}$ layer that mixes with the surface will act as a further $CO_2$ sink. Several reports indicate deepening of the surface mixed layer by strong wind with the passage of low pressure systems and their biogeochemical impacts (Wada et al., 2011; Rumyantseva et al., 2015). Simmonds and Keay (2009) reported that the strength of cyclones in the Arctic Ocean is increasing with the long-term reduction of sea-ice cover. However, we must consider the strength of stratification in the Canada Basin. In a comprehensive analysis of mixed layer depth in the Arctic Ocean, Peralta-Ferriz et al. (2015) found a significant positive correlation (4.6 ± 0.8 m per m $sec^{-1}$) between the mixed layer depth and the maximum wind speed in the preceding 5 days in the case of differences in density between the mixed layer and 20 m below it ($\Delta\rho$) being smaller than 0.5 kg $m^{-3}$. In the case of $\Delta\rho$ > 0.5 kg $m^{-3}$, deepening of the mixed layer accompanying the increase in wind speed was almost zero (0.77 ± 0.52 m per m $sec^{-1}$). In our observations, $\Delta\rho$ exceeded 2.0 kg $m^{-3}$ at all CTD stations in the Canada Basin (Fig. 4c). Hence, we think that additional $CO_2$ uptake in the Canada Basin by wind mixing is unlikely because stratification was strong even in 2013 and will be strengthened by further input of sea-ice melt in the future.

Climate change also affects the subsurface layer in the Canada Basin, where low $pCO_2^{sea}$ is caused by net primary production. McLaughlin and Carmack (2010) reported that increase in sea-ice melt and the strengthening of Ekman pumping

deepened the nutricline and the depth of chlorophyll maximum in the Canada Basin. Nishino et al. (2013) also observed decreases in nitrate and chlorophyll in the 0 to 50 m depth layer in the Canada Basin during 2002–2010; they attributed these decreases to the decrease in inflow of nutrient-rich water from the East Siberia Sea. In any case, biological production below the halocline of the Canada Basin is likely to decrease in the long term. In this regard, it seems unlikely that the subsurface low $pCO_2^{sea}$ layer in the Canada Basin will act as another $CO_2$ sink.

## 4. Conclusions

A wide range of surface $pCO_2^{sea}$ was observed in the western Arctic Ocean in September 2013. The value was as low as 180 µatm in the Chukchi Sea where biological activity was high in early summer. In contrast, $pCO_2^{sea}$ in the Canada Basin in September reached 360 µatm, almost equivalent to $pCO_2^{air}$. Based on our use of salinity and TA to identify the fraction of freshwater, we attributed the low salinity in the Canada Basin to sea-ice melt. Large input of oligotrophic sea-ice melt not only inhibits biological activity, but also forms a thin surface mixed layer that easily reaches equilibrium with atmospheric $CO_2$. In the area where riverine output was more dominant than sea-ice melt, the increase in $pCO_2^{sea}$ was indistinct due to the input of riverine nutrients and TA. Although both meltwater and river water are freshwater, the effects of riverine output differed from those of sea-ice melt.

In the Canada Basin a strong halocline (density gradient > 2.0 kg $m^{-3}$) was formed under the surface mixed layer, where $pCO_2^{sea}$ was the lowest (~250 µatm); this differs from other regions where $pCO_2^{sea}$ was lowest at the surface. This subsurface $pCO_2^{sea}$ minimum corresponded to rWML and PSW and is attributable to net primary production. The subsurface low $pCO_2^{sea}$ layer in the Canada Basin has a potential to absorb atmospheric $CO_2$ in case it is transported to the surface by vertical mixing. However, such a $CO_2$ sink is unlikely because this stratification is strong enough to resist vertical mixing by wind. Additionally, long-term observations in the Canada Basin suggest that subsurface biological activity has been declining in recent decades.

Our observations revealed only a part of the complex carbon cycle in the Arctic Ocean. The subsurface $pCO_2^{sea}$ minimum is peculiar to the Canada Basin, where a complicated water column structure exists; these results are unlikely to be applicable to the entire Arctic Ocean. In the changing Arctic Ocean, although these subregional variations and processes are essential for accurate projections of the future carbon cycle, they are not adequately reflected in current models. Observable areas in the Arctic Ocean are expected to expand along with long-term sea-ice retreat. Comprehensive observations are essential especially in such areas because sea-ice melt may cause other unknown effects.

## References

Anderson, L. G., Jutterström, S., Kaltin, S., Jones, E. P., and Björk, G. : Variability in river runoff distribution in the Eurasian Basin of the Arctic Ocean, J. Geophys. Res., 109, C01016, doi:10.1029/2003JC001773, 2004.

Bates, N. R.: Air-sea $CO_2$ fluxes and the continental shelf pump of carbon in the Chukchi Sea adjacent to the Arctic Ocean, J. Geophys. Res., 111, C10013, doi:10.1029/2005JC003083, 2006.

Bates, N. R. and Mathis, J. T.: The Arctic Ocean marine carbon cycle: Evaluation of air-sea $CO_2$ exchanges, ocean acidification impacts and potential feedbacks, Biogeosciences, 6, 2433–2459, doi:10.5194/bg-6-2433-2009, 2009.

Bates, N. R., Garley, R., Frey, K. E., Shake, K. L., and Mathis, J. T.: Sea-ice melt $CO_2$–carbonate chemistry in the western Arctic Ocean: meltwater contributions to air–sea $CO_2$ gas exchange, mixed-layer properties and rates of net community production under sea ice, Biogeosciences, 11, 6769-6789, doi:10.5194/bg-11-6769-2014, 2014.

Behrenfeld, M. J. and Falkowski, P. G.: A consumers guide to phytoplankton primary production models, Limnol. Oceanogr., 42(7), 1479–1491, 1997.

Cai, W.-J., Chen, L., Chen, B., Gao, Z., Lee, S.H., Chen, J., Pierrot, D., Sullivan, K., Wang, Y., Hu, X., Huang, W.-J., Zhang, Y., Xu, S., Murata, A., Grebmeier, J. M., Jones, E. P., and Zhang, H.: Decrease in the $CO_2$ uptake capacity in an ice-free Arctic Ocean basin, Science, 329, 556–559, doi:10.1126/science.1189338, 2010.

Comiso, J.: Large decadal decline of the Arctic multiyear ice cover, J. Clim., 25, 1176–1193, doi:10.1175/JCLI-D-11-00113.1, 2012.

Cooper, L. W., McClelland, J. W., Holmes, R. M., Raymond, P. A. Gibson, J. J., Guay, C. K., and Peterson, B. J.: Flow-weighted values of runoff tracers ($\delta^{18}O$, DOC, Ba, alkalinity) from the six largest Arctic rivers, Geophys. Res. Lett., 35, L18606, doi:10.1029/2008GL035007, 2008.

Déry, S. J., Hernández-Henríquez, M. A., Burford, J. E., and Wood, E. F.: Observational evidence of an intensifying hydrological cycle in northern Canada, Geophys. Res. Lett., 36, L13402, doi:10.1029/2009GL038852, 2009.

Dickson, A.G.: Determination of dissolved oxygen in sea water by Winkler titration, in WHP Operations and Methods. WHP Office Report Woods Hole, Massachusetts, USA, pp. 1–14, 1994.

Dickson, A. G., Sabine, C. L., and Christian, J. R.: Guide to best practices for ocean $CO_2$ measurements, Sidney, British Columbia, North Pacific Marine Science Organization, PICES Special Publication 3, 2007.

Else, B. G. T., Galley, R. J., Lansard, B., Barder, D. G., Brown, K., Miller, L. A., Mucci, A., Papakyriakou, T. N. Tremblay, J.-É., and Rysgaard, S.: Further observations of a decreasing atmospheric $CO_2$ uptake capacity in the Canada Basin (Arctic Ocean) due to sea ice loss, Geophys. Res. Lett., 40, 1132–1137, doi:10.1002/grl.50268, 2013.

Fransson, A., Chierici, M., and Nojiri, Y.: New insights into the spatial variability of the surface water carbon dioxide in varying sea ice conditions in the Arctic Ocean, Cont. Shelf Res., 29, 1317–1328, doi:10.1016/j.csr.2009.03.008, 2009.

Fransson, A., Chierici, M., Miller, L. A., Carnat, G., Shadwick, E., Thomas, H., Pineault, S., and Papakyriakou, T. N.: Impact of sea-ice processes on the carbonate system and ocean acidification at the ice-water interface of the Amundsen Gulf, Arctic Ocean, J. Geophys. Res. Oceans, 118, 7001–7023, doi:10.1002/2013JC009164, 2013.

Hsu, S. A., Meindl, E. A, and Gilhousen, D. B.: Determining the power-law wind-profile exponent under near-neutral stability conditions at sea, J. Appl. Meteorol., 33, 757 – 765, 1994.

Jackson, J. M., Carmack, E. C., McLaughlin, F. A., Allen, S. E., and Ingram, R. G.: Identification, characterization, and change of the near-surface temperature maximum in the Canada Basin, 1993–2008, J. Geophys. Res., 115, C05021, doi:10.1029/2009JC005265, 2010.

Laruelle, G. G., Lauerwald, R., Pfeil, B., and Regnier, P.: Regionalized global budget of the $CO_2$ exchange at the air-water interface in continental shelf seas, Global Biogeochem. Cycles, 28, 1199–1214, doi:10.1002/2014GB004832, 2014.

Lee, S. H., Stockwell, D. A., Joo, H.-M., Son, Y. B., Kang, C.-K., and Whitledge, T. E.: Phytoplankton production from melting ponds on Arctic sea ice, J. Geophys. Res., 117, C04030, doi:10.1029/2011JC007717, 2012.

Le Quéré, C., Andrew, R. M., Canadell, J. G., Sitch, S., Korsbakken, J. I., Peters, G. P., Manning, A. C., Boden, T. A., Tans, P. P., Houghton, R. A., Keeling, R. F., Alin, S., Andrews, O. D., Anthoni, P., Barbero, L., Bopp, L., Chevallier, F., Chini, L. P., Ciais, P., Currie, K., Delire, C., Doney, S. C., Friedlingstein, P., Gkritzalis, T., Harris, I., Hauck, J., Haverd, V., Hoppema, M., Klein Goldewijk, K., Jain, A. K., Kato, E., Körtzinger, A., Landschützer, P., Lefèvre, N., Lenton, A., Lienert, S., Lombardozzi, D., Melton, J. R., Metzl, N., Millero, F., Monteiro, P. M. S., Munro, D. R., Nabel, J. E. M. S., Nakaoka, S.-I., O'Brien, K., Olsen, A., Omar, A. M., Ono, T., Pierrot, D., Poulter, B., Rödenbeck, C., Salisbury, J., Schuster, U., Schwinger, J., Séférian, R., Skjelvan, I., Stocker, B. D., Sutton, A. J., Takahashi, T., Tian, H., Tilbrook, B., van der Laan-Luijkx, I. T., van der Werf, G. R., Viovy, N., Walker, A. P., Wiltshire, A. J., and Zaehle, S.: Global Carbon Budget 2016, Earth Syst. Sci. Data, 8, 605-649, doi:10.5194/essd-8-605-2016, 2016.

Lueker, T. J., Dickson, A. G., and Keeling, C. D.: Ocean $pCO_2$ calculated from dissolved inorganic carbon, alkalinity, and equations for $K_1$ and $K_2$: Validation based on laboratory measurements of $CO_2$ in gas and seawater in equilibrium, Mar. Chem., 70, 105–119, 2000.

Manizza, M., Follows, M. J., Dutkiewicz, S., Menemenlis, D., Hill, C. N., and Key, R. M.: Changes in the Arctic Ocean $CO_2$ sink (1996–2007): A regional model analysis, Global Biogeochem. Cycles, 27, 1108–1118, doi:10.1002/2012GB004491, 2013.

Martin, J., Tremblay, J.-É., Gagnon, J., Tremblay, G., Lapoussiére, A., Jose, C., Poulin, M., Gosselin, M., Gratton, Y., and Michel, C.: Prevalence, structure and properties of subsurface chlorophyll maxima in Canadian Arctic waters, Mar. Ecol. Prog. Ser., 412, 69–84, doi:10.3354/meps08666, 2010.

McClelland, J. W., Déry, S. J., Peterson, B. J., Holmes, R. M., and Wood, E. F.: A pan-arctic evaluation of changes in river discharge during the latter half of the 20th century, Geophys. Res. Lett., 33, L06715, doi:10.1029/2006GL025753, 2006.

McLaughlin, F. A. and Carmack, E. C.: Deepening of the nutricline and chlorophyll maximum in the Canada Basin interior, 2003–2009, Geophys. Res. Lett., 37, L24602, doi:10.1029/2010GL045459, 2010.

Mirorikawa, T., Ishii, M., Nemoto, K., Kamiya, H., Nakadate, A., Masuda, S., Matsueda, H., Nakano, T., and Inoue, H. Y.: Interannual variability of winter oceanic $CO_2$ and air-sea $CO_2$ flux in the western North Pacific for 2 decades, J. Geophys. Res., 111, C07S02, doi:10.1029/2005JC003095, 2006.

Nishino, S., Itoh, M., Williams, W. J., and Semiletov, I.: Shoaling of the nutricline with an increase in near-freezing temperature water in the Makarov Basin, J. Geophys. Res. Oceans, 118, 635–649, doi:10.1029/2012JC008234, 2013.

Nishino, S., Kawaguchi, Y., Inoue, J., Hirawake, T., Fujiwara, A., Futsuki, R., Onodera, J., and Aoyama, M.: Nutrient supply and biological response to wind-induced mixing, inertial motion, internal waves, and currents in the northern Chukchi Sea, J. Geophys. Res. Oceans, 120, 1975–1992, doi:10.1002/2014JC010407, 2015.

Parkinson, C. L. and Comiso, J. C.: On the 2012 record low Arctic sea ice cover: Combined impact of preconditioning and an August storm, Geophys. Res. Lett., 40, 1356–1361, doi:10.1002/grl.50349, 2013.

Peralta-Ferriz, C. and Woodgate, R. A.: Seasonal and interannual variability of pan-Arctic surface mixed layer properties from 1979 to 2012 from hydrographic data, and the dominance of stratification for multiyear mixed layer depth shoaling, Prog. Oceanogr., 134, 19–53, doi:10.1016/j.pocean.2014.12.005, 2015.

Rabe, B., Karcher, M., Kauker, F., Schauer, U., Toole, J. M., Krishfield, R. A., Pisarev, S., Kikuchi, T., and Su, J.: Arctic Ocean basin liquid freshwater storage trend 1992–2012, Geophys. Res. Lett., 41, 961–968, doi:10.1002/2013GL058121, 2014.

Rumyantseva, A., Lucas, N., Rippeth, T., Martin, A, Painter, S. C., Boyd, T. J., and Henson, S.: Ocean nutrient pathways associated with the passage of a storm, Global Biogeochem. Cycles, 29, 1179–1189, doi:10.1002/2015GB005097, 2015.

Rysgaard, S., Glud, R. N., Sejr, M. K., Bendtsen, J., and Christensen, P. B.: Inorganic carbon transport during sea ice growth and decay: A carbon pump in polar seas, J. Geophys. Res., 112, C03016, doi:10.1029/2006JC003572, 2007.

Shimada, K., Itoh, M., Nishino, S., McLaughlin, F., Carmack, E., and Proshutinsky A.: Halocline structure in the Canada Basin of the Arctic Ocean, Geophys. Res. Lett., 32, L03605, doi:10.1029/2004GL021358, 2005.

Simmonds, I., and Keay, K.: Extraordinary September Arctic sea ice reductions and their relationships with storm behavior over 1979–2008, Geophys. Res. Lett., 36, L19715, doi:10.1029/2009GL039810, 2009.

Steele, M., Morison, J., Ermold, W., Rigor, I., Ortmeyer, M., and Shimada, K.: Circulation of summer Pacific halocline water in the Arctic Ocean, J. Geophys. Res., 109, C02027, doi:10.1029/2003JC002009, 2004.

Stroeve, J. C., Kattsov V., Barrett, A., Serreze, M., Pavlova, T., Holland, M., and Meiner, W. N.: Trends in Arctic sea ice extent from CMIP5, CMIP3 and observations, Geophys. Res. Lett., 39, L16502, doi:10.1029/2012GL052676, 2012a.

Stroeve, J. C., Serreze, M. C., Holland, M. M., Kay, J. E., Malanik, J., and Barrett, A. P.: The Arctic's rapidly shrinking sea ice cover: A research synthesis, Clim. Change, 110, 1005–1027, doi:10.1007/s10584-011-0101-1, 2012b.

Takahashi, T., Sutherland, S. C., Wanninkhof, R., Sweeney, C., Feely, R. A., Chipman, D. W., Hales, B., Friederich, G., Chavez, F., Sabine, C., Watson, A., Bakker, D. C. E., Schuster, U., Metzl, N., Yoshikawa-Inoue, H., Ishii, M., Midorikawa, T., Nojiri, Y., Kortzinger, A., Steinhoff, T., Hoppema, M., Olafsson, J., Arnarson, T. S., Tilbrook, B., Johannessen, T., Olsen, A., Bellerby, R., Wong, C. S., Delille, B., Bates, N. R., and de Baar, H. J. W: Climatological mean and decadal change in surface ocean $pCO_2$, and net sea-air $CO_2$ flux over the global oceans, Deep Sea Res., Part II, 56(8–10), 554–577, doi:10.1016/j.dsr2.2008.12.009, 2009.

Ulfsbo, A., Cassar, N., Korhonen, M., van Heuven, S., Hoppema, M., Kattner, G., and Anderson, L. G.: Late summer net community production in the central Arctic Ocean using multiple approaches, Global Biogeochem. Cycles, 28, 1129–1148, doi:10.1002/2014GB004833, 2014.

Wada, A., Midorikawa, T., Ishii, M., and Motoi, T.: Carbon system changes in the East China Sea induced by Typhoons Tina and Winnie in 1997, J. Geophys. Res., 116, C07014, doi:10.1029/2010JC006701, 2011.

Wanninkhof, R. H.: Relationship between wind speed and gas exchange over the ocean, J. Geophys. Res., 97, 7373–7382, 1992.

Weiss, R. F.: Carbon dioxide in water and seawater: The solubility of a non-ideal gas, Mar. Chem., 2, 203–215, 1974.

Yamamoto-Kawai, M., Tanaka, N., and Pivovarov, S.: Freshwater and brine behaviors in the Arctic Ocean deduced from historical data of $\delta^{18}O$ and alkalinity (1929–2002 A.D.), J. Geophys. Res., 110, C10003, doi:10.1029/2004JC002793, 2005.

Yamamoto-Kawai, M., McLaughlin, F. A., Carmack, E. C., Nishino, S. Shimada, K., and Kurita, N.: Surface freshening of the Canada Basin, 2003–2007: River runoff versus sea ice meltwater, J. Geophys. Res., 114, C00A05, doi:10.1029/2008JC005000, 2009.

Yao, W. S. and Byrne, R. H.: Simplified seawater alkalinity analysis: Use of linear array spectrometers, Deep Sea Res., Part I, 45(8), 1383–1392, doi:10.1016/S0967-0637(98)00018-1, 1998.

Biogeosciences Discuss., doi:10.5194/bg-2017-148, 2017
Manuscript under review for journal Biogeosciences
Discussion started: 21 April 2017


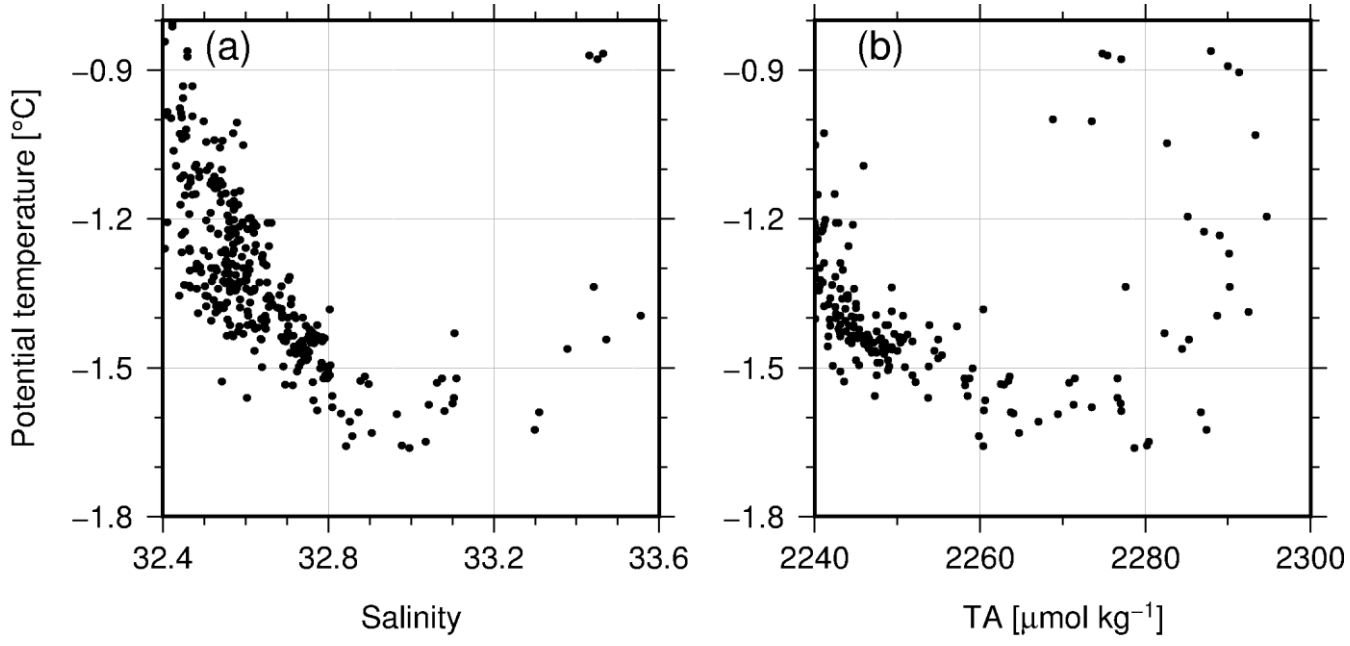


**Figure 1: Water properties around the temperature minimum layer in the Chukchi Sea and the Canada Basin in samples collected during cruise MR13-06 from 3 September to 1 October 2013. Potential temperature versus (a) salinity and (b) total alkalinity (TA).**

Biogeosciences Discuss., doi:10.5194/bg-2017-148, 2017
Manuscript under review for journal Biogeosciences
Discussion started: 21 April 2017


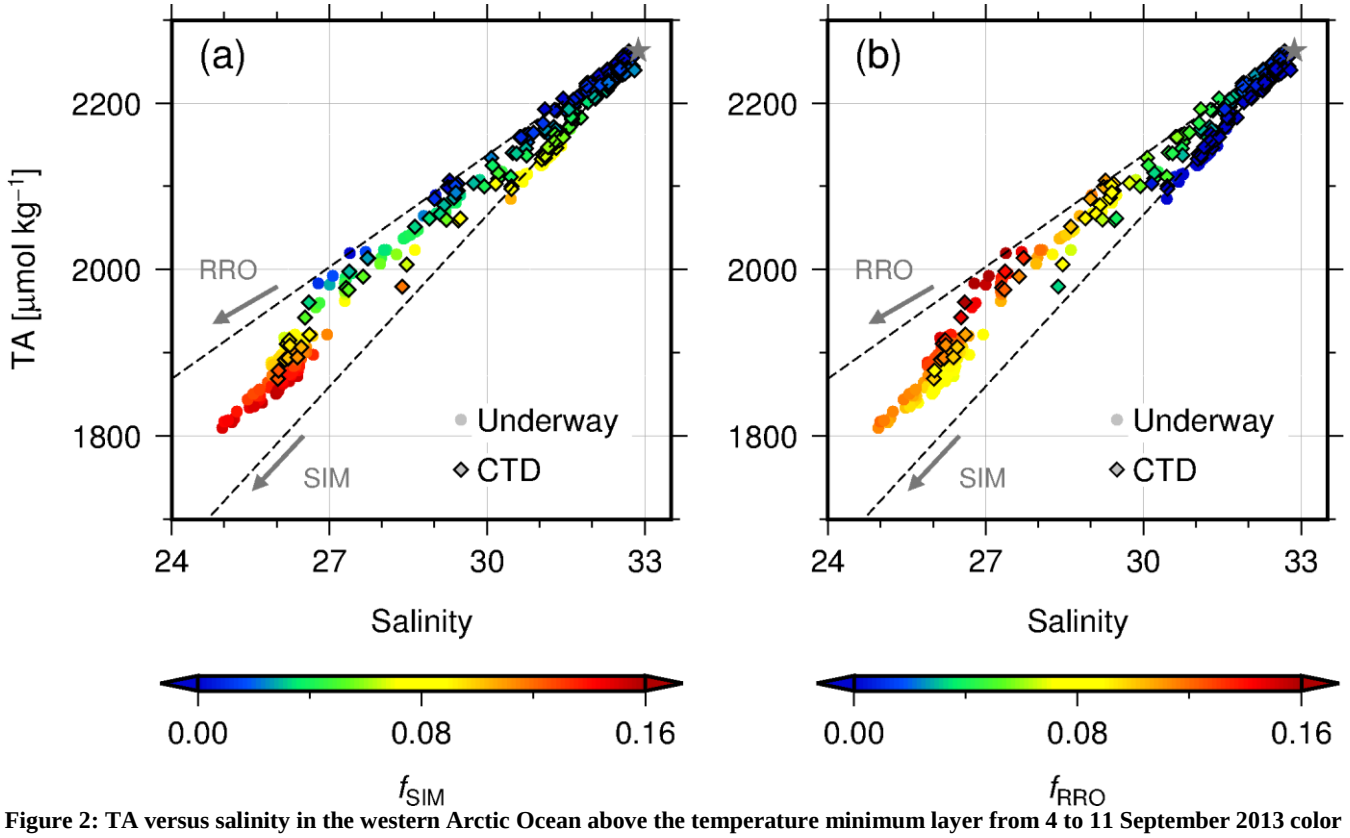


**Figure 2: TA versus salinity in the western Arctic Ocean above the temperature minimum layer from 4 to 11 September 2013 color coded for (a) the fraction of sea-ice melt ($f_{SIM}$) and (b) the fraction of riverine outflow ($f_{RRO}$). Circles and diamonds denote surface water and CTD samples, respectively. Star denotes the salinity and TA of Pacific origin water (POW: $S$ = 32.89 and TA = 2264.2 µmol kg$^{-1}$). Broken lines extend to the two endmembers, sea-ice melt (SIM: $S$ = 5 and TA = 349 µmol kg$^{-1}$) and riverine output (RRO: $S$ = 0 and TA = 793 µmol kg$^{-1}$).**

Biogeosciences Discuss., doi:10.5194/bg-2017-148, 2017
Manuscript under review for journal Biogeosciences
Discussion started: 21 April 2017


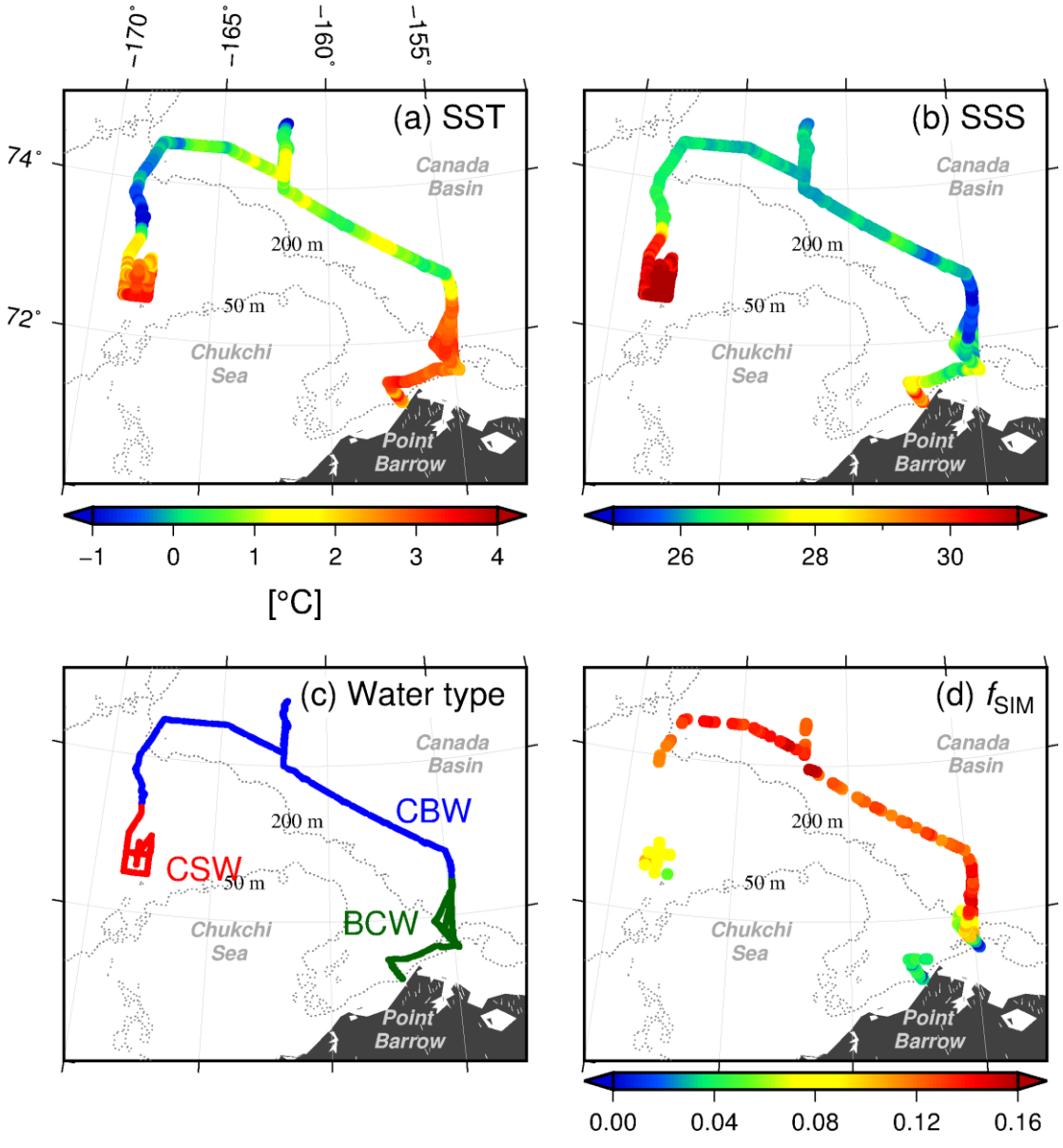


**Figure 3: Surface water properties along the track of cruise MR13-06 from 4 to 11 September 2013. (a) Sea surface temperature (SST), (b) sea surface salinity (SSS), (c) BCW (Barrow Coastal Water), CSW (Chukchi Sea Water), and CBW (Canada Basin Water) water type according to SST and SSS, (d) $f_{SIM}$, (e) $f_{RRO}$, (f) $pCO_2^{sea}$, (g) $nDIC_{32}$ = DIC / *S* * 32; DIC normalized to *S* =32 and (h) $nTA_{32}$ = TA / *S* * 32; TA normalized to *S* =32 . Dotted lines indicate 50 and 200 m isodepths.**

Biogeosciences Discuss., doi:10.5194/bg-2017-148, 2017
Manuscript under review for journal Biogeosciences
Discussion started: 21 April 2017


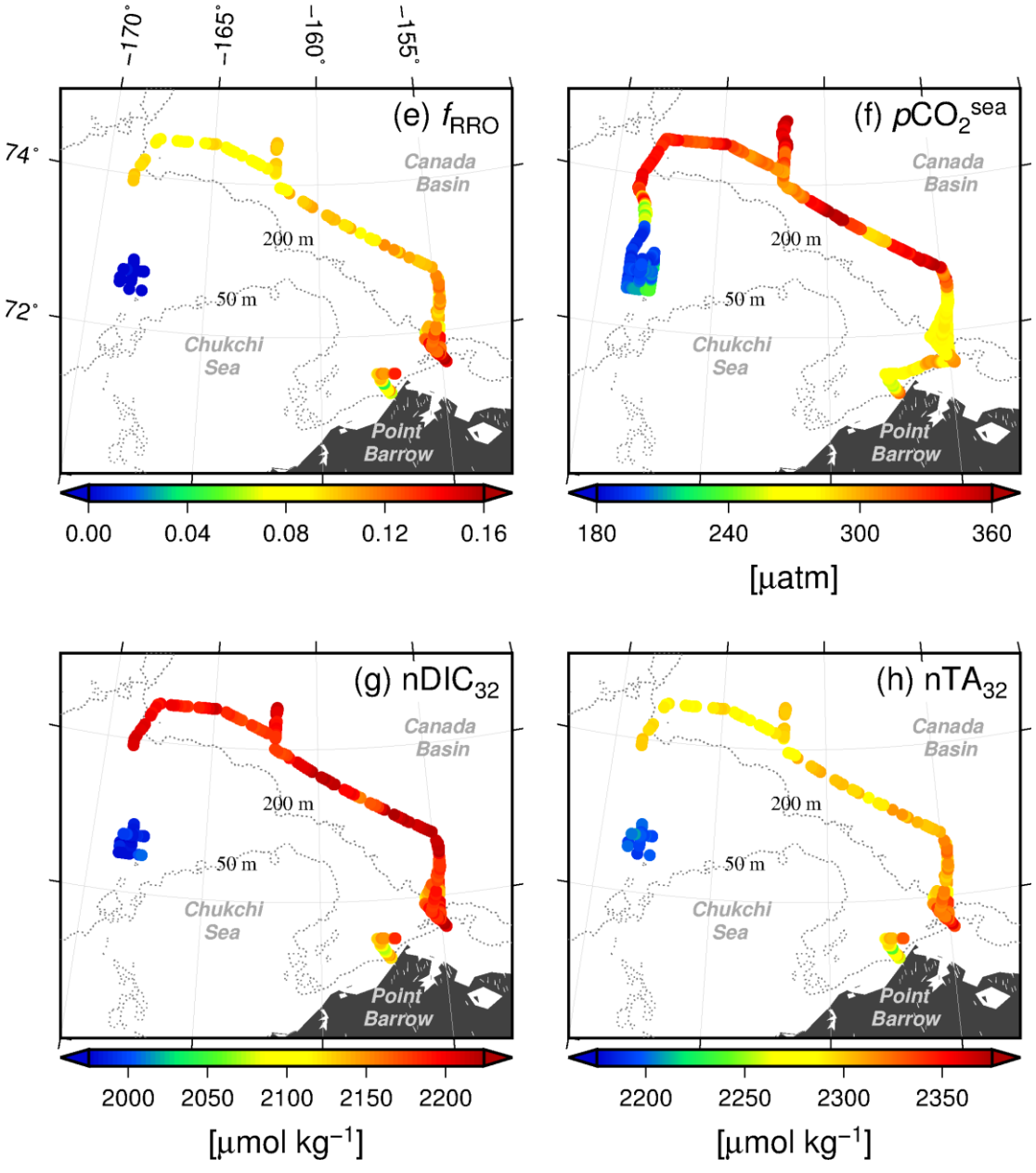


**Figure 3 (continued)**

Biogeosciences Discuss., doi:10.5194/bg-2017-148, 2017
Manuscript under review for journal Biogeosciences
Discussion started: 21 April 2017


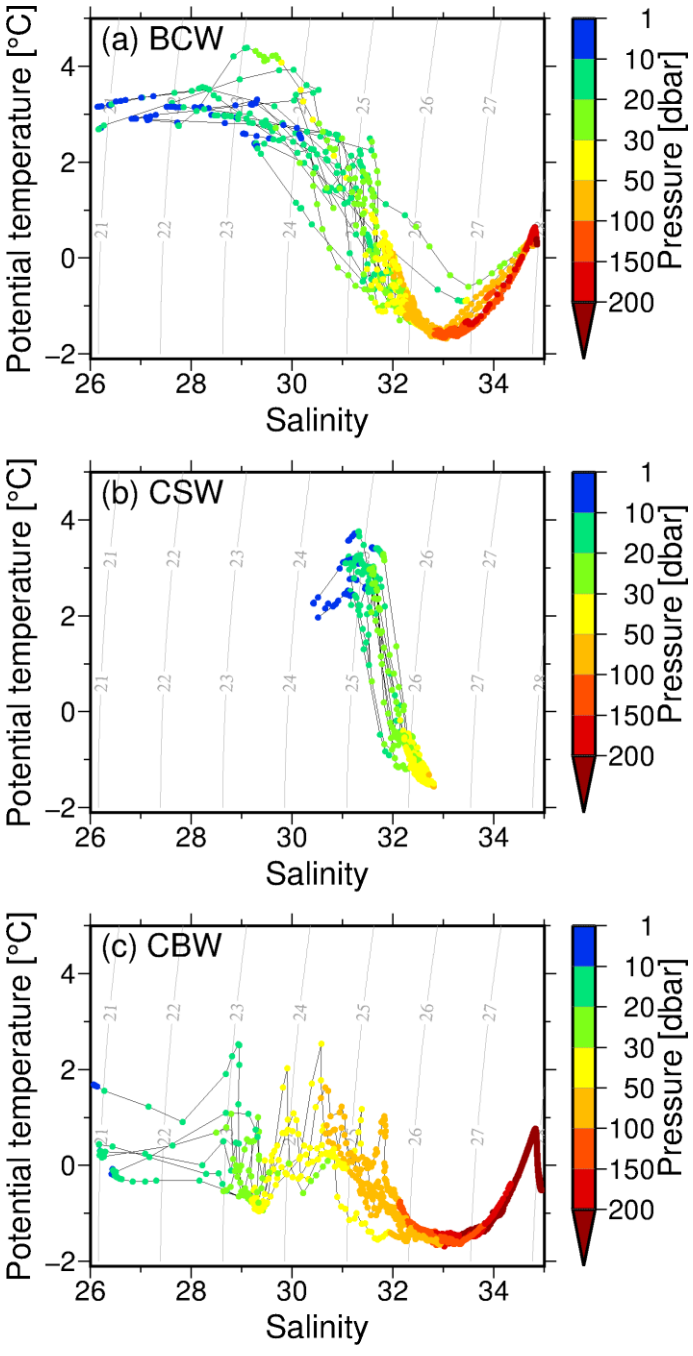


**Figure 4: Column salinity and potential temperature in (a) BCW (Barrow Coastal Water), (b) CSW (Chukchi Sea Water), and (c) CBW (Canada Basin Water). Water pressure is indicated by color. Gray contours indicate potential density ($\sigma_\theta$ = {density – 1} × 1000 [kg m$^{-3}$]).**

Biogeosciences Discuss., doi:10.5194/bg-2017-148, 2017
Manuscript under review for journal Biogeosciences
Discussion started: 21 April 2017


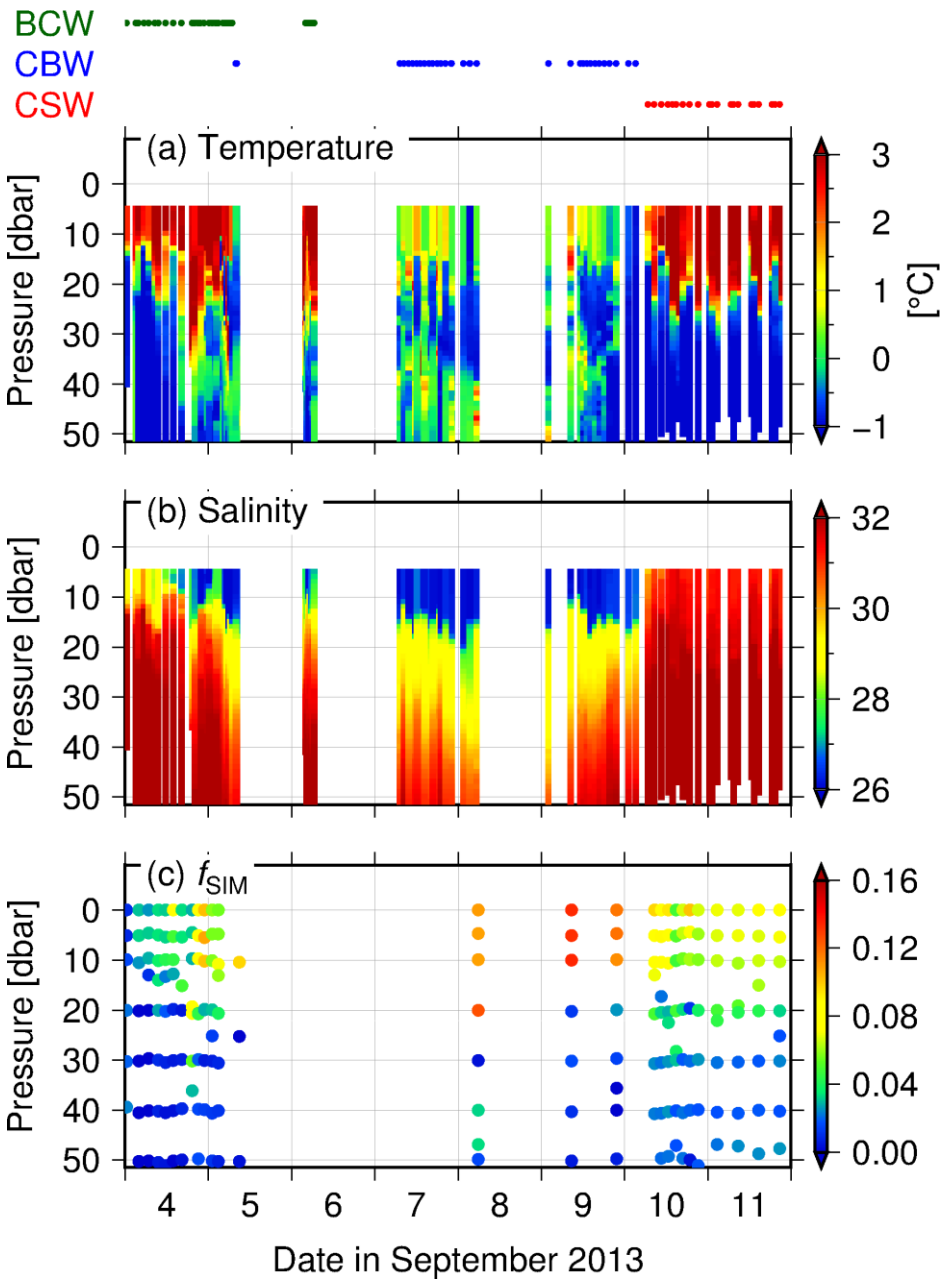


**Figure 5: Column profiles of (a) temperature, (b) salinity, (c) $f_{SIM}$, (d) $f_{RRO}$, (e) $pCO_2^{sea}$, and (f) apparent oxygen utilization (AOU) along the cruise track in the period 4–11 September 2013. Water types BCW (Barrow Coastal Water, CBW (Canada Basin Water), and CSW (Chukchi Sea Water) are indicated at the top of the figure.**

Biogeosciences Discuss., doi:10.5194/bg-2017-148, 2017
Manuscript under review for journal Biogeosciences
Discussion started: 21 April 2017


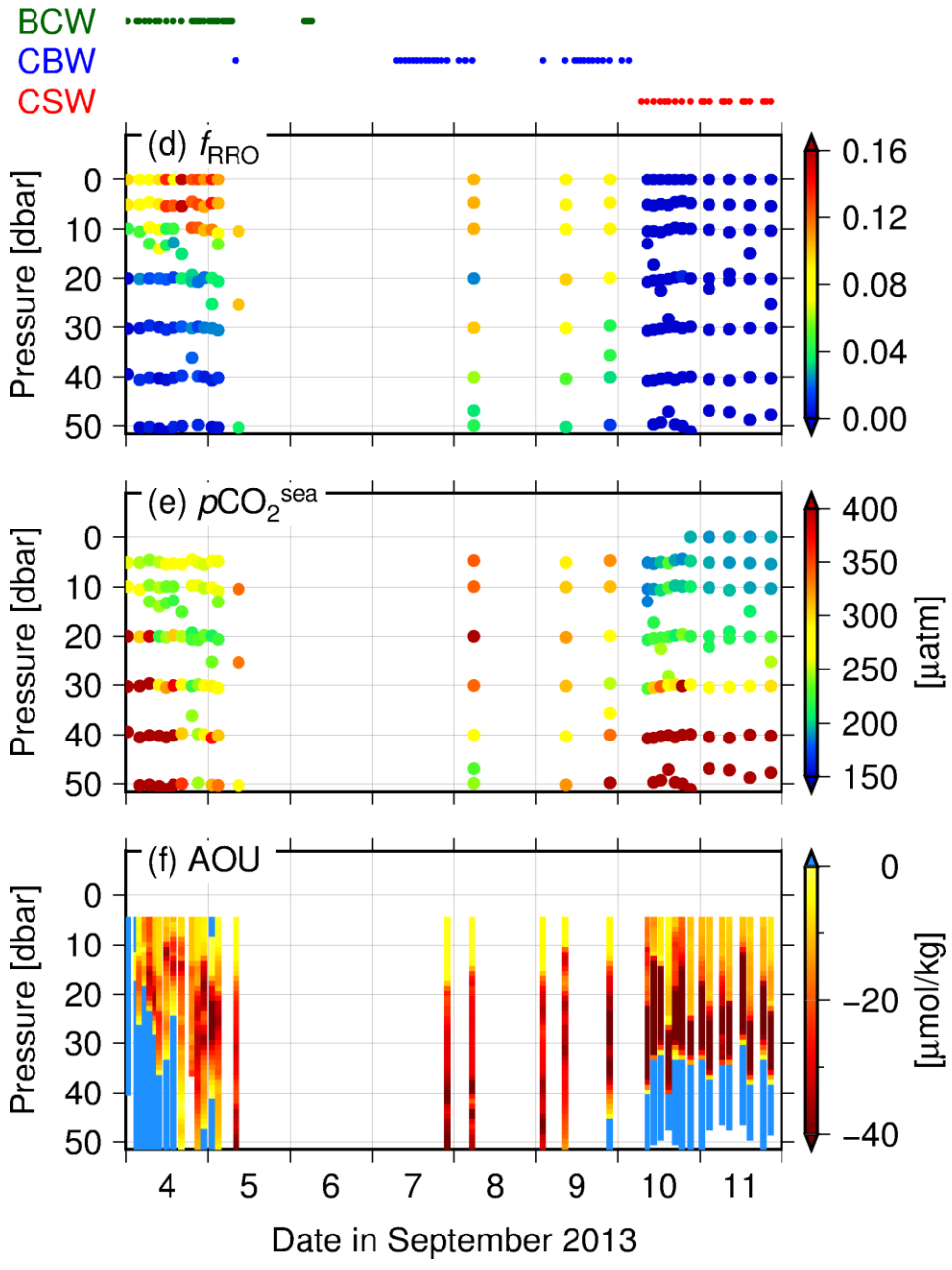


**Figure 5 (continued)**

Biogeosciences Discuss., doi:10.5194/bg-2017-148, 2017
Manuscript under review for journal Biogeosciences
Discussion started: 21 April 2017


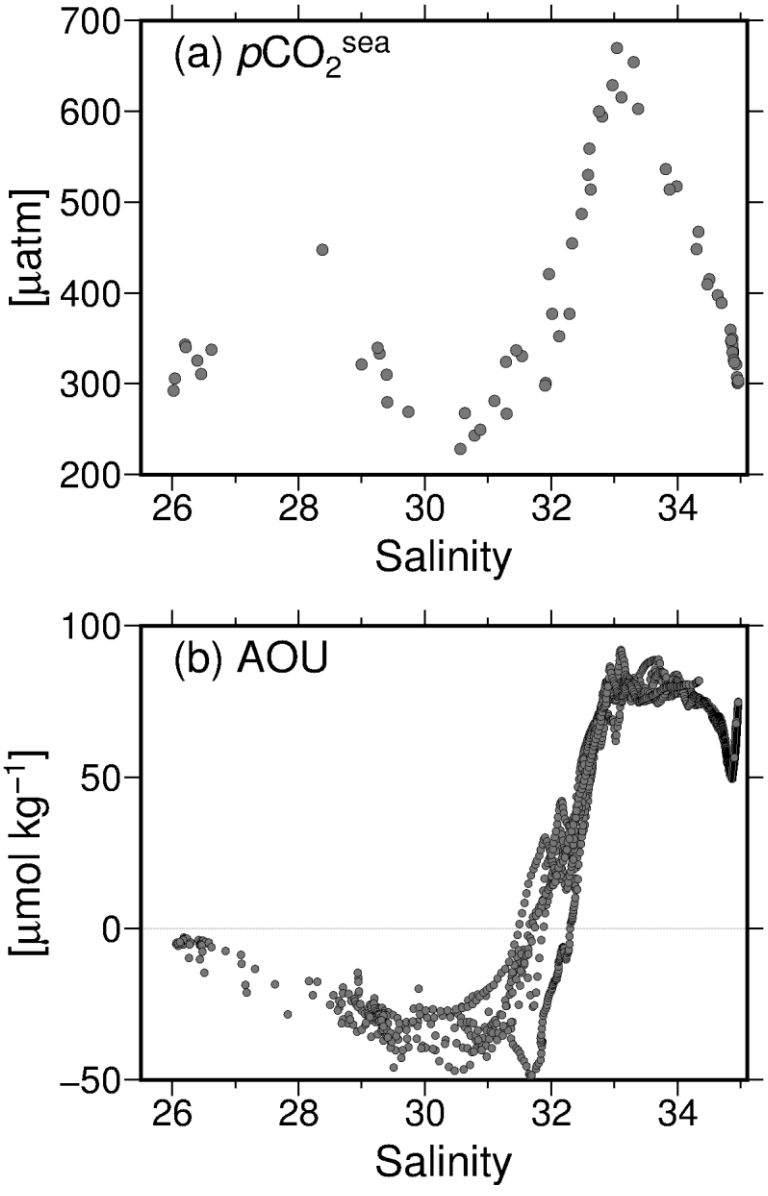


**Figure 6: Canada Basin Water values for (a) salinity and $pCO_2^{sea}$ in discrete bottle samples and (b) salinity and apparent oxygen utilization (AOU) from CTD cast data.**

Biogeosciences Discuss., doi:10.5194/bg-2017-148, 2017
Manuscript under review for journal Biogeosciences
Discussion started: 21 April 2017


**Table 1: Summary of three water types (BCW, Barrow Coastal Water; CBW, Canada Basin Water; and CSW, Chukchi Sea Water) in the western Arctic Ocean. Values are averages for samples collected from 4 to 11 September 2013. N denotes the number of samples. $nDIC_{32}$ and $nTA_{32}$ are DIC and TA normalized to *S* =32 respectively ($nDIC_{32}$ = DIC / *S* * 32; $nTA_{32}$ = TA / *S* * 32).**

| Water type | N | T [°C] | S | DIC [μmol kg$^{-1}$] | $nDIC_{32}$ [μmol kg$^{-1}$] | TA [μmol kg$^{-1}$] | $nTA_{32}$ [μmol kg$^{-1}$] | DIC/TA | $pCO_2^{sea}$ [μatm] | $f_{SIM}$ | $f_{RRO}$ |
|---|---|---|---|---|---|---|---|---|---|---|---|
| BCW | 109 | 2.88 | 27.01 | 1827 | 2166 | 1948 | 2309 | 0.938 | 274 | 0.11 | 0.08 |
| CBW | 118 | 0.66 | 26.19 | 1803 | 2203 | 1882 | 2299 | 0.958 | 332 | 0.10 | 0.12 |
| CSW | 54 | 3.03 | 31.06 | 1923 | 1982 | 2131 | 2196 | 0.903 | 198 | –0.01 | 0.08 |